Journal of
Materials Chemistry C

Accepted Manuscript

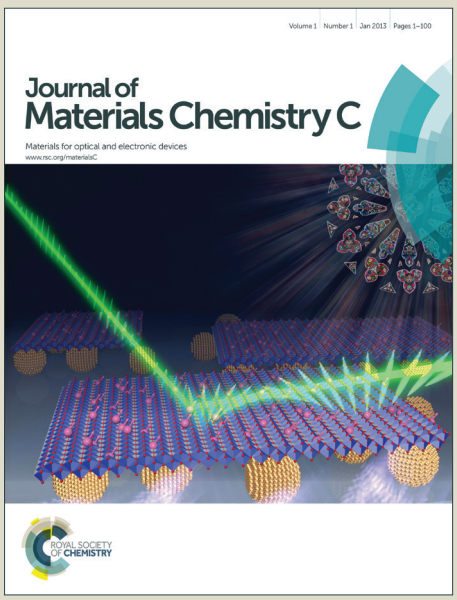

ROYAL SOCIETY OF CHEMISTRY

www.rsc.org/materialsC

Synthesis, Electronic Structures and Luminescent Properties of Eu^{3+} Doped $KGdTiO_4$

Niumiao Zhang, Chongfeng Guo*, Jiming Zheng, Xiangying Su, Jin Zhao

National Key Laboratory of Photoelectric Technology and Functional Materials (Culture Base) in Shaanxi Province, National Photoelectric Technology and Functional Materials & Application of Science and Technology International Cooperation Base, Institute of Photonics & Photon-Technology, Northwest University, Xi'an 710069, China;

Author to whom correspondence should be addressed

E-mail: guocf@nwu.edu.cn (Prof. Guo);

Tel & Fax: ±86-29-88302661

Abstract

Eu^{3+}-activated layered perovskite ionic conductor $KGdTiO_4$ red emitting phosphors used for ultraviolet based light emitting diodes (LEDs) and field emission displays (FEDs) were successfully synthesized by a modified sol-gel method. The electronic structure of $KGdTiO_4$ was estimated by the density functional theory (DFT) calculation. The phase purity and luminescent properties of samples were characterized by x-ray diffraction (XRD), photoluminescence excitation (PLE) and emission (PL) spectra. The cathode-luminescence (CL) spectra of phosphors as function of accelerating voltage and filament current were also measured. In addition, the thermal stability phosphors are investigated according to the temperature-dependent PL spectra and the decay curves. The Eu^{3+} doped $KGdTiO_4$ phosphor offers higher brightness and thermal stability, which shows great potential application in LEDs and FEDs as a suitable red-emitting phosphor candidate.

Keywords: Potoluminescence; Cathoeluminescence; Phosphor.

1. Introduction

Recently, phosphors have undergone an unprecedented development due to the emergence of new materials and technologies, such as GaN-based blue light-emitting diodes (LEDs), field emission displays (FEDs), plasma display panels (PDPs) and so on. White light emitting diodes (w-LEDs) are recognized as a light source for next-generation owing to their energy saving, high efficiency, long lifetime and environmentally friendly characteristics. Now, white LEDs are generally fabricated by the combination of blue or *ultraviolet chip* with phosphors, but stable and efficient red or orange emitting phosphors are short. As one of the most promising technologies for flat panel display, FEDs are realized by phosphors under low-voltage (≤5 kV) and high current density (10-100 μA/cm^2) excitation of high energy electron *bombardment* [1-2]. In above mentioned two devices, red-emitting phosphor is requisite and phosphor Y_2O_2S: Eu^{3+} is still traditionally used as red light components in both devices. However, *the stabilities of sulfide-based phosphors are poor* under the excitation of the UV high energy photon or electron bombardment, which seriously lowers the luminous efficiency of the phosphors and deteriorates the performances of devices [3-4]. To overcome these problems, it is urgent to develop novel red phosphors with satisfactory stability and high luminance. In comparison with sulfides, Eu^{3+} doped oxide-based red emitting have been investigated extensively for their easy preparation, eco-friendly, strong absorption in the near-ultraviolet region, effective energy transfer from the host lattice to the activator Eu^{3+} ions, and impressive chemical and physical stability [5-6]. *Layered* perovskite structures oxide compounds have been paid more attention due to their strong direct excitation bands and higher activator critical concentration [7]. As a member of compounds with layered perovskite structure, complex oxides $ALnTiO_4$ (A includes alkaline metal, Ag and other monovalent ions, Ln=rare earth) contains ordered A-site cations, *therefore these compounds are typical ionic conductor. Moreover, these compounds are suitable systems to investigate luminescent properties of two-dimensional compounds, in which the concentration of dopant is higher than others because each Ln ion has four Ln neighbors via 180° interactions and eight Ln neighbors via double 90° interactions* [8-9].

It is well known that the electrical conductivity of phosphors should be high enough to avoid charge accumulation in the applications of FEDs. Usually, there are two methods to enhance the conductivity of phosphor: one of the methods is to decrease the particle grain size; the other

method is to choose a conductor as host. Most researches are focused on the former, but no related reports have been published for the latter [10-11]. In comparison with traditional solid state reaction, products prepared with sol-gel method offer high purity, low reaction temperature and higher photo-luminescent intensity, which are favorable to its applications in UV LEDs and FEDs [12-13]. Hence, Eu^{3+} doped layered perovskite titanates compound $KGdTiO_4$ red emitting phosphors were synthesized using a sol-gel method, and the structure, thermal stability, photoluminescent and cathodoluminescent properties of phosphors have also been studied.

2. Experimental

2.1 Synthesis of samples

Red emitting phosphor $KGdTiO_4:Eu^{3+}$ were synthesized by sol-gel method and the raw materials include analytical reagent (A.R.) K_2CO_3, $Ti(OC_4H_9)_4$ and rare earth oxides Gd_2O_3, Eu_2O_3 with high purity (99.99%). In addition, analytical reagent CH_3CH_2OH and CH_3COOH were also used as solvent and hydrolysis inhibitor in this experiment, respectively. First, the stoichiometric amount of rare earth oxides Ln_2O_3 (Ln = Eu or Gd) and K_2CO_3 (excess 30% as flux) were dissolved in dilute HNO_3 and the excess HNO_3 was volatilized at high temperature. Then, transparent solution A was obtained by adding a certain amount of deionized water into the above mixture. The calculated volume of acetic acid, ethanol and $Ti(OC_4H_9)_4$ were mixed to form the plained and transparent solution B. Subsequently, solution B was added drop-wise to solution A with constant stirring to obtain the final plained and transparent solution. The final plained and transparent solution was dried in an oven at 70 □ for 24 hours and 120 □ for 24 h in order until white dried gel was formed. Finally, the dried gel was grinded and pre-heated in furnace at 500 □ for 2 h and then sintered at the temperature from 700 to 1100 □ for 3 h with 100 □ interval to obtain the required samples.

2.2 Characterization

The powder X-ray diffractions (XRD) of samples were carried out by using a Rigaku-Dmax 3C powder diffract meter with Cu-Kα (λ=1.5405 Å) radiation in the range of $10^0 \leqq 2\theta \leqq 60^0$. The photoluminescence excitation (PLE) and photoluminescence (PL) spectra were measured with a Hitachi F-7000 fluorescence spectrophotometer equipped with a 150 W xenon lamp as excitation

source. *Quantum efficiency was measured using the integrating sphere on the FLS 920 fluorescence spectrometer, and a 450 W xenon lamp was used as the excitation source and white $BaSO_4$ powder as a reference.* The dependence of PL spectra on temperature and luminescence decay curves were characterized using *the same Edinburgh FLS 920 spectrometer* combined fluorescence lifetime. The cathode-luminescence (CL) measurements were tested in a vacuum chamber (10^{-4} Pa), in which the phosphors were excited by the electron beam at a voltage from 0.5 to 4 kV and the filament currents from 50-120 μA. The CL spectra were recorded by a spectrometer (Ocean Optics QEB0388) with a charge coupled device (CCD) camera through an optical fiber.

2.3 Computational details

To investigate the electronic structures of pure $KGdTiO_4$, calculations were performed in the density functional theory (DFT) framework using the Vienna *ab-initio* simulation package (VASP). Projector-augmented-wave (PAW) potentials were used to explain the electron-ion interactions, while the exchange correlation effects were treated within the generalized gradient approximation (GGA) under the scheme of Perdew-Burke-Ernzerhof (PBE). *The self-consistent field (SCF) energy convergence threshold is set as 0.02eV/Å to ensure the accuracy of the electronic calculation.* The kinetic energy cutoff was set at 600 eV, and a *k*-point sampling 7×7×3 Monkhorst-Pack mesh was used. The lattice constants a_1, a_2, a_3 were used after geometry relaxation, which is similar to the crystal structure determined by XRD measurements.

3. Results and discussion

3.1 Phase purity and crystal structure

In present systems, Eu^{3+} ions are expected to occupy the sites of Gd^{3+} due to their same valence and close radius, thus the nominal formula of the samples could be expressed as $KGd_{1-x}Eu_xTiO_4$. The phase purity and the crystal structure of samples were identified by the powder X-ray diffraction pattern (XRD). All samples are prepared at 800 ℃ for 6 h because the pure phase and brightest emission. *Fig. 1a* representatively shows the XRD patterns of the $KGdTiO_4$ samples as a function of the dopant Eu^{3+} concentration in a range of *10*-100 mol %. The XRD patterns of all samples are similar in our experiments. It is found that all diffraction peaks are in good agreement with those of $KGdTiO_4$ in Ref.14 and no detectable impurity phase appeared. Results indicate that

the introduction of the dopants Eu^{3+} does not cause any significant change for the host structure and Eu^{3+} ions have completely entered the host lattice. As Gd^{3+} ions were completely substituted by Eu^{3+} ions, the compound $KEuTiO_4$ is successfully synthesized and shares the same crystal structure with $KGdTiO_4$. Structurally, the compound $KGdTiO_4$ belongs to orthorhombic system with the space group *Pbcm* (57) and its crystal structure diagram plotted with Diamond 3.1 (as shown in *Fig. 1b*), which has a layered structure. The Ti-O layers are interspersed by K-O double layers and the Gd-O, which offers more interspaces for K^+ ions to move to strengthen the conductivity.

3.2 Electronic structure

The electronic structure of $KGdTiO_4$ was investigated by the first principle calculation using VASAP code, and the calculated band structures of pure $KGdTiO_4$ is shown in *Fig. 2*. The results reveal that the pure $KGdTiO_4$ is a direct band-gap of approximately 3.04 eV with the valence bands maximum (VBM) and the conduction bands minimum located at the same Γ point. It can be concluded that the $KGdTiO_4$ is a suitable host for luminescence materials with a wide band gap between 3.0-6.0 eV), and could accommodate both the group and excited states of dopant ions within the band gap [15]. However, the calculated band gap is inconstant with the experimental optical band gap of about 4.32 eV. The large difference between the calculated and experimental value in the band gaps is probably attributed to two main reasons [16]. The first one is that the DFT approximation (GGA) always underestimates the band gaps; the other one is that the fundamental absorption edge of the prepared $KGdTiO_4$ powder is located in the range of 220-290nm which is already within lower-limit of our UV/Vis machine.

The density of states (DOS) of $KGdTiO_4$ was calculated and shown in *Fig. 3*, which is favorable to understand the composition of the energy bands. It is clearly observed that the valence band is composed of dominant O 2*p* and small contribution from Ti 3*d* states ranging from -5 eV to the Fermi level (set as 0 eV). While the conduction band (just above the Fermi level) in $KGdTiO_4$ ranging from 3.04 eV to 7.0 eV is mainly formed by Ti-3*d* states and a slight contribution of the Gd-4*d* and O-2*p*. These results provide the useful information of the host lattice which is helpful to understand the luminescence phenomenon that the host absorptions at low energy region can be mainly ascribed to the charge transitions from O-2*p* to Ti-3*d* states.

As discussed above, the host absorption of $KGdTiO_4$ can be mainly ascribed to the charge

transitions from O-2*p* to Ti-3*d* states. However, there are sixteen oxygen atoms in the unit cell of $KGdTiO_4$, as shown in *Fig. 4b*. According to their different symmetry, perovskite layered *properties* and bonding environments of $KGdTiO_4$, the sixteen oxygen atoms could be classified into four types due to their different sites. Among four different oxygen groups, which O-site does make more contribution at the valence band maximum? In order to answer this question, the partial density of states (PDOSs) of the four types O-site in $KGdTiO_4$ were calculated and shown in *Fig. 4a*. It is clear *shown* that the O_3 *dominate* the valence band maximum, mixing with very small amount of O_2 and O_1 between -2 and 0 eV. So we can further identify the interband optical transition is mainly from O_3-2*p* states and Ti-3*d* states.

3.3 Luminescent properties of samples at RT.

Fig. 5 shows the excitation and emission spectra of $KGdTiO_4$:$x$$Eu^{3+}$ phosphors with various Eu^{3+} concentrations (x). As shown in *Fig. 5a*, all excitation spectra monitoring at the dominant emission wavelength peaked at 617 nm are composed of a broad band in shorter wavelength ranging from 220 to 350 nm and a group of sharp lines absorption in 350-500 nm longer-wavelength region. The former broad band absorption should attribute to the possible overlap between the charge transfer band of O^{2-}-Eu^{3+} and the host lattice (TiO_4^{4-} group) [3]. It indicates that the host $KGdTiO_4$ could *absorb* the excitation energy and then transfer the energy to the activator ions Eu^{3+}. The other part of sharp lines absorption at 363, 383, 395, 416 and 465 nm are assigned the $^7F_0 \rightarrow {}^5D_4$, $^7F_0 \rightarrow {}^5L_7$, $^7F_0 \rightarrow {}^5L_6$, $^7F_0 \rightarrow {}^5D_3$ and $^7F_0 \rightarrow {}^5D_2$ transitions of Eu^{3+}, respectively. The excitation peaks at 395 and 465 nm match well with the commercial InGaN-based near UV or blue LED chips, which implies that the present phosphors have potential application in W-LEDs [17]. The emission spectra of samples $KGdTiO_4$:$x$$Eu^{3+}$ excited with 286 and 395 nm are similar except relative intensities, thus only PL spectra excited at 286 nm are representatively shown in *Fig. 5b*. All emission spectra consist of several sharp lines emission peaked at 580, 590, 617, 652 and 700 nm, respectively, and they *come* from the transitions from the excited $^5D_0$ level to ^7F_J (J=0, 1, 2, 3, 4) levels of Eu^{3+} [18, 19]. Among these emission lines, the peak at 617 nm from the electric dipole transition $^5D_0$-$^7F_2$ of Eu^{3+} dominates the emission spectra, which *indicates* that Eu^{3+} ions occupy the sites without centro-symmetry. Generally, the electric-dipole (ED) emission $^5D_0$-$^7F_2$ of Eu^{3+} is hypersensitive, while the magnetic-dipole (MD) emission $^5D_0$-$^7F_1$ is insensitive to the crystal field environment. If there is no inversion symmetry at the site of Eu^{3+}, the ED transitions are no longer

strictly forbidden; even for small deviations from inversion symmetry, they will appear dominantly in the PL spectrum [20]. Therefore, the intensity ratio value (R) of the transition *from* $^5D_0$-$^7F_2$ to $^5D_0$-$^7F_1$ (R=I_{ED}/I_{MD}) is a good parameter to measure the extent of distortion from the inversion symmetry of the Eu^{3+} site, where I is usually defined the integrated area under their PL curves. In present systems, the R values for all samples are beyond 1.8, indicating that Eu^{3+} occupies a site without centro-symmetry, which is in agreement with above mentioned.

Inset of *Fig. 5b* shows the dependence of PL intensity (the integrated area under the PL profile from 525 to 725 nm) on the contents of Eu^{3+}. It is clearly found that the PL intensity increased firstly and then decreased after reaching the optimal concentration of Eu^{3+} at x = 0.3 due to the concentration quenching effect. In this compound $KGdTiO_4$, its critical concentration is higher than those of other inorganic phosphors, which due to the energy transfer is restricted to quasi-two-dimensional Eu^{3+} sub-lattice in the layered perovskite compound [21]. Generally, concentration quenching occurs as a result of non-radiative energy transfer among luminescent centers, and the critical distance between the luminescent centers is an appropriate parameter. The probability of energy transfer between two activators is inversely proportional to the nth power of the distance of the activators [22]. With the increase of Eu^{3+} concentration, the distance between Eu^{3+} ions *becomes* smaller and the probability of energy transfer increases [23]. The concentration quenching will not exist if the average distance between the neighboring Eu^{3+} ions is beyond the critical distance (Rc), which is the shortest distance between the nearest activator ions and can be calculated from the following formula [24, 25]:

$$R_C \approx 2 \times \left(\frac{3V}{4\pi X_c N}\right)^{1/3} \qquad (1)$$

Where N is the number of Z ions in the unit cell if the activator is introduced solely on Z ion sites, X_c is the critical concentration, and V is the volume of the unit cell. According to previous publications [6, 25] and our above results, the value of V, N and X_c is 380.6×10^{-30} m^3, 4 and 0.3, respectively. The critical distance R_C between the Eu^{3+} ions in the $KGdTiO_4$:Eu^{3+} was calculated to be 8.46 Å. According to the Blasse's theory [26], if the Eu^{3+}–Eu^{3+} distance is larger than 5 Å, exchange interaction becomes ineffective and only the multipolar interactions are of importance; whereas, exchange interaction becomes effective. Accordingly, Rc is overe 5 Å, the luminescence of the phosphors will be efficient at room temperature, such as the $EuAl_3B_4O_{12}$ (Eu^{3+}–Eu^{3+} 5.9 Å),

$Eu(IO_3)_3$ (Eu^{3+}–Eu^{3+} 5.9 Å) and $CsEuW_2O_8$ (Eu^{3+}–Eu^{3+} 5.2 Å) [27]. In this case, the critical distance *Rc* (8.46 Å) between Eu^{3+} in compound $KGdTiO_4$ is much larger than 5 Å, which is too large to shift for the energy transfer and leading to the high concentration quenching in the $KGdTiO_4$:Eu^{3+}. *The quantum efficiency of the sample $KGd_{0.7}Eu_{0.3}TiO_4$ with optimal composition has been measured to be 91% with 395 nm excitation at room temperature, which is close or over some commercial red phosphor. Results indicate that the present phosphor is a good red emitting phosphor candidate for LED.*

Fig. 6 portrays the PL spectra of $KGd_{0.7}Eu_{0.3}TiO_4$ phosphors with their corresponding color coordinates (inset) under 286 nm excitation. The CIE chromaticity coordinate of $KGd_{0.7}Eu_{0.3}TiO_4$ was calculated to be (0.65, 0.34) according to its PL spectrum, which is close to that of the NTSC standard CIE chromaticity coordinate value for red (0.67, 0.33) and superior to those of commercial red phosphors Y_2O_2S: Eu^{3+} (0.65, 0.36) and Y_2O_3:Eu^{3+} (0.49, 0.32) [13,28]. In addition, the photograph in *Fig. 6* presents the red emission of phosphor $KGd_{0.7}Eu_{0.3}TiO_4$ under a 254 nm UV lamp, which also implies that the phosphor could be an outstanding red-emitting phosphor.

3.4 Thermal Stabilities of samples

As we all know, the thermal stability is one of the key technological issues for phosphors applied in LEDs and FEDs [29, 30]. In most cases, the temperature dependence of phosphors is a decisive factor for thermal stability owing to its considerable influence on the CIE coordinates and efficiency of phosphor. *Fig. 7a* presents the PL *spectrum* of $KGd_{0.7}Eu_{0.3}TiO_4$ with optimal composition as a function of temperature under the excitation of 395 nm UV light. It observed that the PL profiles of the sample at different temperatures are similar and no significant shifts except tiny decreases in the PL intensity with the increase of temperature. The dependence of the normalized integrated PL intensity of the phosphor on the temperature is portrayed in *Fig. 7b*, in which the PL intensity decreases with increasing the temperature and reaches to about 89% and 81% of the room temperature (300 K) at 100 and 200 ℃, respectively. Results indicate that the $KGd_{0.7}Eu_{0.3}TiO_4$ phosphor offers outstanding thermal stability, which further proves the present phosphor is excellent red emitting phosphor candidate for the application in LEDs and FEDs.

For further characterizing the stability of the present phosphor $KGd_{0.7}Eu_{0.3}TiO_4$, the temperature dependent PL lifetimes of Eu^{3+} at 617 nm under the excitation of 395 nm in the range

of 298 to 473 K are depicted in *Fig. 7c*. It is *found* that the PL lifetimes slightly decrease with the increase of temperature, which due to the decrease of the lifetimes of the excited states with increasing temperature as a result of a substantial increase in non-radiative relaxation rate [31,32]. The lifetime could be calculated by the fitting into a single exponential equation $I = I_0 \exp[-t/\tau]$, where I is the luminescence intensity at the time t, I_0 is the initial emission intensity for $t = 0$, τ is the decay time for the exponential components. The value of τ was calculated to be about 1.15 ms at room temperature (298 K) and the lifetime close to a constant with increasing temperature from 323 to 423 K, which further *indicates* that the $KGdTiO_4:Eu^{3+}$ phosphors have an excellent thermally stability on temperature quenching effects. Accordingly, in order to investigate the characteristics of thermal quenching, the activation energy could be calculated according to the Arrhenius equation, which has been given as the following formula: [33, 34]

$$I(T) = \frac{I_0}{1 + c\exp(-E_a/kT)} \qquad (3)$$

where I_0 is the initial intensity of the phosphor *at the temperature* $T \rightarrow 0K$, $I(T)$ is the intensity of the phosphor at a certain temperature T, c is a constant, E_a is the activation energy for thermal quenching, and k is Boltzmann's constant (8.62×10^{-5} eV/K). *Here, the value of* I_0 *was used that of at 3.5K, which is reasonable for the calculation.* According to *equation* (3), the plot of $\ln[(I_0/I) - 1]$ *vs*. 10000/T yields a straight line, as shown in *Fig. 7d*. Through the best fit, the experimentally activation energy E_a was obtained as *0.08eV* for $KGd_{0.7}Eu_{0.3}TiO_4$.

3.5 CL spectra of samples

In order to explore the potential application of red emitting phosphor $KGd_{0.7}Eu_{0.3}TiO_4$ in FED, its cathode-luminescence (CL) property *has* been investigated. *Fig. 8a* displays the CL spectrum of $KGd_{0.7}Eu_{0.3}TiO_4$ under the low-voltage electron bean excitation (accelerating voltage: 3 kV and filament current 30 μA), which is identical to the PL *spectrum*. *Fig. 8b* and c show the dependences of CL emission intensities for $KGd_{0.7}Eu_{0.3}TiO_4$ on the accelerating voltage and filament current. When the filament current is fixed at 30 μA, the CL intensity gradually increases with raising the accelerating voltage from 0.5 to 4.0 kV (as shown in *Fig. 8b*). Similarly, under a 3.0 kV electron beam excitation, the CL intensity also increases with increasing the filament

current from 50 to 100 μA and then shows saturation with filament current beyond 100 μA (*Fig. 8c*). However, there is no obvious saturation effect for the CL intensity with the increase of accelerating voltage. For cathode-luminescence, the Eu^{3+} ions are excited by the plasmons produced by the incident electrons. More plasma was produced with the increase of accelerating voltage and filament current, resulting in more Eu^{3+} ions excited and intense CL emission [35]. In addition, the increase in CL brightness is attributed to the deeper penetration of the electrons into the phosphor body and the larger electron-beam current density. The electron penetration depth can be estimated using the empirical formula: [36]

$$L\ (\text{Å}) = 250\ (A/\rho)(E/Z^{1/2})^{n} \qquad (4)$$

where $n = 1.2\ /(1\text{-}0.29\log Z)$, A is the atomic or molecular weight of the materials, ρ is the bulk density, Z is the atomic number or the number of electrons per molecule in the case of compounds, and E is the accelerating voltage (kV).The higher accelerating voltage and filament current, the larger the energy of the accelerating electron and so the deeper penetration depth.[37]. Results indicate that $KGd_{0.7}Eu_{0.3}TiO_4$ offers excellent CL property and is a potential red light emitting phosphor for FED devices.

4. Conclusions

In conclusion, a series of Eu^{3+} doped ionic conductor $KGdTiO_4$ red emitting phosphors have been successfully synthesized by sol-gel method. Electronic structure of the host was analyzed using the calculation of the density of states (DOS), results indicate that the direct band gap for $KGdTiO_4$ is about 3.04 eV and the host absorption is mainly ascribed to the charge *transition* from O-2*p* to Ti-3*d* states. The Eu^{3+} ion doped $KGdTiO_4$ phosphors show bright PL and CL red emission under UV excitation and high energy electron beam excitation. The optimal composition for the present phosphors is 30 % Eu^{3+} doping concentration and heated at 800 ℃ for 6 h, its CIE coordinate (0.65, 0.34) is close to the NTSC standard CIE chromaticity coordinate. Moreover, the present *phosphors* show superior thermal stability, the PL intensity at 200 ℃ is over 80% of the room temperature, and no significant shift for the emission spectra and CIE coordinates. Our results display that Eu^{3+} doped $KGdTiO_4$ is excellent red emitting candidates for LEDs and FEDs.

Acknowledgements

This work was supported by the high-level talent project of Northwest University, National Natural Science Foundation of China (No. 11274251), Ph.D. Programs Foundation of Ministry of Education of China (20136101110017), Technology Foundation for Selected Overseas Chinese Scholar, Ministry of Personnel of China (excellent), Foundation of Key Laboratory of Photoelectric Technology in Shaanxi Province (12JS094) and the Open Foundation of Key Laboratory of Photoelectric Technology and Functional Materials (Culture Base) in Shaanxi Province (ZS11010, ZS12020), NWU Graduate Innovation and Creativity Funds (YZZ12028).

References

[1] X. G. Xu, J. Chen, S. Z. Deng, N. S. Xu, H. B Liang, Q. Su and J. Lin, High luminescent Li_2CaSiO_4: Eu^{2+} cyan phosphor film for wide color gamut field emission display, *Optics Express*, 2012, **20**, 17701-17710.

[2] C.C. Kang and R.S. Liu, The effect of terbium concentration on the luminescent properties of yttrium oxysulfide phosphor for FED application, *J. Luminescence*, 2007, **122–123**, 574–576.

[3] C. F. Guo, D. X. Huang and Qiang Su, Methods to improve the fluorescence intensity of CaS: Eu^{2+} red emitting phosphor for white LED, *Materials Science and Engineering B*, 2006, **130**, 189-193.

[4] B. L. Abrams and P. H. Holloway, Role of the surface in luminescent processes, *Chemical Reviews*, 2004, **104**, 5783-5801.

[5] S. H. Park, K. H. Lee, S. Unithrattil, H. S. Yoon, H. G. Jang and W. B. Im, Melilite-structure $CaYAl_3O_7$:Eu^{3+} phosphor: Structural and optical characteristics for near-UV LED-based white light, *J. Phys. Chem. C*, 2012, **116**, 26850-26856.

[6] N. M. Zhang, C. F Guo and H. Jing, Photoluminescence and Cathode-luminescence of Eu^{3+} doped $NaLnTiO_4$ (Ln = Gd and Y) Phosphors, *RSC adv*., 2013, **3**, 7495-7502.

[7] T. S. Chan, C. L. Dong, Y. H. Chen, Y. T Lu, S.Y. Wu, Y. R. Ma, C.C. Lin, R. S. Liu, J. L. Chen, J. H. Guo, J. F. Lee, H. S. Sheu, C. C. Yang and C. L. Chen, Mechanism of light emission and electronic properties of a Eu^{3+}-doped $Bi_2SrTa_2O_9$ system determined by coupled X-ray absorption and emission spectroscopy, *J. Mater. Chem.*, 2011, **21**, 17119-17127.

[8] K. Toda, Y. Kameo, S. Kurita and M. Sato, Crystal structure determination and ionic conductivity of layered perovskite compounds $NaLnTiO_4$ (Ln=rare earth), *J. Alloys and Compounds*, 1996, **234**, 19-25.

[9] *G. Blasse and A. Bril, Fluorescence of Eu^{3+}-activated sodium lanthanide titanates ($NaLn_{1-x}Eu_xTiO_4$), J. Chem. Physics, 1968,* ***48****, 3652–3656.*

[10] P. Psuja, D. Hreniak and W. Strek, Rare earth doped nanocrystalline phosphors for field emission displays, *J. Nanomater*, 2007, **2007**, 81350.

[11] G. S. R. Raju, Y. H. Ko, E. Pavitra, J. S. Yu, J. Y. Park, H. C. Jung and B. K. Moon, Formation of $Ca_2Gd_8(SiO_4)_6O_2$ nanorod bundles based on crystal splitting by mixed solvothermal and hydrothermal reaction methods, *Crystal Growth & Design*, 2012, **12**, 960–969.

[12] R. P. Rao, Preparation and characterization of fine-grain yttrium-based phosphors by sol-gel method, *J. Electrochem. Soc*., 1996, **143**, 189-197.

[13] C. F. Guo, W. Zhang, L. Luan, T. Chen, H. Cheng and D. X. Huang, A promising red-emitting phosphor for

White Light emitting diodes prepared by sol-gel method, *Sensors and Actuators B*, 2008, **133**, 33-39.

[14] R. E. Schaak and T. E. Mallouk, $KLnTiO_4$(Ln =La, Nd, Sm, Eu, Gd, Dy): A New Series of Ruddlesden-Popper Phases Synthesized by Ion-Exchange of $HLnTiO_4$, *J. Solid State Chemistry*, 2001, **161**, 225-232.

[15] Y. C. Jia, H. Qiao, N. Guo, Y. H. Zheng, M. Yang, Y. J. Huang and H. P. You, Electronic structure and photoluminescence properties of Eu^{2+}-activated $Ca_4Si_2O_7F_2$, *Optical Materials*, 2011, **33**, 1803-1807.

[16] Y. Q. Li, N. Hirosaki, R. J. Xie, T. Takeka and M. Mitpmo, Crystal, electronic structures and photoluminescence properties of rare-earth doped $LiSi_2N_3$, *J. Solid State Chemistry*, 2009, **182**, 301-311.

[17] Y. Tian, X. H. Qi, X. W. Wu, R. N. Hua and B. J. Chen, Luminescent Properties of $Y_2(MoO_4)_3$: Eu^{3+} Red Phosphors with Flowerlike Shape Prepared via Coprecipitation Method, *J. Phys. Chem. C* 2009, **113**, 10767-10772.

[18] N. J. Cockroft and J. C. Wright, Local- and distant-charge compensation of Eu^{3+} ions in defect centers of $SrTiO_3$, *Phys. Rev. B*, 1992, **45**, 9642-9655.

[19] A. Patra, E. Sominska, S. Ramesh, Y. Koltypin, Z. Zhong, H. Minti, R. Reisfeld and A. Gedanken, Sonochemical preparation and Characterization of Eu_2O_3 and Tb_2O_3 Doped in and Coated on Silica and Alumina Nanoparticles, *J. Phys. Chem. B*, 1999, **103**, 3361-3365.

[20] C. F. Guo, X. Ding and Y. Xu, Luminescent properties of Eu^{3+}-doped $BaLn_2ZnO_5$ (Ln=La, Gd and Y) phosphors by sol-gel method, *J. American Ceramic Soc*., 2010, **93**, 1708-1713.

[21] K. Tezuka, Y. Hinatsu, N. M. Masaki and M. Saeki, Magnetic Properties of Layered Perovskites Na*Ln*TiO_4(*Ln*=Sm, Eu, and Gd), *J. Solid State Chemistry*, 1998, **138**, 342-346.

[22] J. R. Qiu, K. Miura, N. Sugimoto and K. Hirao, Preparation and fluorescence properties of fluoroaluminate glasses containing Eu^{2+} ions, *J. Non-Cryst. Solids*, 1997, **213/214**, 266–270.

[23] B. J. M. Dierre, R. J. Xie, N. Hirosaki and T. Sekiguchi, Blue emission of Ce^{3+} in lanthanide silicon oxynitride phosphors, *J. Mater. Res*., 2007, **22**, 1933–1941.

[24] G. Blasse, Energy transfer in oxide phosphors. *Philps Res. Rep*., 1969, **24**, 131–144.

[25] H. Jing, C. F. Guo, G. G. Zhang, X. Y. Su, Z. Yang and J. H. Jeong. Photoluminescent properties of Ce^{3+} in compounds $Ba_2Ln(BO_3)_2Cl$ (Ln = Gd and Y), *J. Mater. Chem*., 2012, **22**, 13612-13618.

[26] G. Blass and B.C. Grabmaier, Luminescent Materials, Springer-Verlag, Berlin, Heidelberg, 1994, p. 99.

[27] Z. Sun, Q. H. Zhang, Y. G. Li and H. Z. Wang, Thermal stable $La_2Ti_2O_7$:Eu^{3+} phosphors for blue-chip white LEDs with high color rendering index, *J. Alloys and Compounds*, 2010, **506**, 338–342.

[28] H. Jing, C. F. Guo, N. M, Zhang, Z.Y. Ren and J. T. Bai, Effects of Eu^{3+} sites on Photoluminescence in $Ba_2Ln(BO_3)_2Cl$ (Ln = Gd, Y) hosts, *ECS J. Solid State Science and Technology*, 2013, **2**, R1-R4.

[29] K. H. Lee, S. H. Park, H. S. Yoon, Y. Kim, H. G. Jang and W. B. Im Bredigite-structure orthosilicate phosphor as a green component fro white LED: the structural and optical properties, *Optics Expess*, 2012, **20**, 6248-6257.

[30] B. L. Abrams, L. Williams, J. S. Bang and P. H. Holloway, Thermal quenching of cathodoluminescence from ZnS: Ag, Cl powder phosphors, *J. Appl. Phys*., 2005, **97**, 033521.

[31] A. Meijerink and G. Blasse, Luminescence and temperature dependent decay behavior of divalent europium in $Ba_5SiO_4X_6$ (X= Cl, Br), *J. Lumin*., 1990, **47**, 1-5.

[32] X. Zhang, F. Meng, H. Wei and H. J. Seo, Eu^{3+} luminescence in novel garnet-type $Li_5La_3Nb_2O_{12}$ ceramics, *Ceramics International*, 2013, **39**, 4063-4067.

[33] S. Bhushan and M. V. Chukichev, Temperature dependent studies of cathodoluminescence of green band of ZnO crystals, *J. Mater. Sci. Lett*., 1988, **7**, 319–321.

[34] Y. H. Chen, B. Liu, C. S. Shi, G. H. Ren and G. Z, The temperature effect of Lu_2SiO_5:Ce^{3+} luminescence, *Nucl. Instrum. Methods Phys. Res. A*, 2005, **537**, 31–35.

[35] X. M. Liu, C. X. Li, Z. W. Quan, Z. Y. Cheng and J. Lin, Tunable luminescence properties of $CaIn_2O_4$:Eu^{3+} phosphors, *J. Phys. Chem. C,* 2007, **111**, 16601-16607.

[36] M. M. Shang, D. L. Geng, X. J. Kang, D. M. Yang, Y. Zhang and J. Lin, Hydrothermal Derived LaOF:Ln^{3+}(Ln = Eu, Tb, Sm, Dy, Tm, and/or Ho) Nanocrystals with Multicolor-Tunable Emission Properties, *Inorg. Chem*., 2012, **51**, 11106-11116.

[37] C. Feldman, Range of 1-10 KeV Electrons in Solids, *Phys. Rev*., 1960, **117**, 455−459.

Figure Captions

Fig.1 XRD patterns of samples $KGd_{1-x}Eu_xTiO_4$ with different Eu^{3+} concentrations (a) annealed at 800 ℃ for 3 h in air and the crystal structure of $KGdTiO_4$ (b).

Fig.2 The calculated energy band structure of $KGdTiO_4$.

Fig.3 Density of states and partial DOS of $KGdTiO_4$ near the Fermi energy level (the Fermi energy is the zero of the energy scale)

Fig.4 Density of states and O-DOS of $KGdTiO_4$ (a), the O-site of $KGdTiO_4$ in unit cell (b).

Fig.5 (a) PLE (λ_{em}= 617 nm) and (b) PL (λ_{ex}=286 nm) spectra of the phosphor $KGdTiO_4$:$x$$Eu^{3+}$ annealed at 800 ℃ for 3 h. Inset is the dependence of the PL intensities on the contents of Eu^{3+} (x).

Fig.6 PL (λ_{ex}=287 nm) spectra of sample $KGd_{0.7}Eu_{0.3}TiO_4$ with its corresponding color coordinates (inset) luminescent photograph (left, *excited at 254 nm*).

Fig.7 Temperature-dependent PL spectra of $KGd_{0.7}Eu_{0.3}TiO_4$ phosphors excited at 395nm (a). Normalized PL intensity of $KGd_{0.7}Eu_{0.3}TiO_4$ phosphors as a function of temperature (b). Decay curves of $KGd_{0.7}Eu_{0.3}TiO_4$ phosphors at different temperatures (c). Plot of $\ln[(I_0/I)-1]$ *vs*. 10000/T for phosphors $KGd_{0.7}Eu_{0.3}TiO_4$ (d).

Fig.8 CL spectra of samples $KGd_{0.7}Eu_{0.3}TiO_4$ (a), the dependence of CL intensity on the accelerating voltage (b) and filament current (c).

Figures

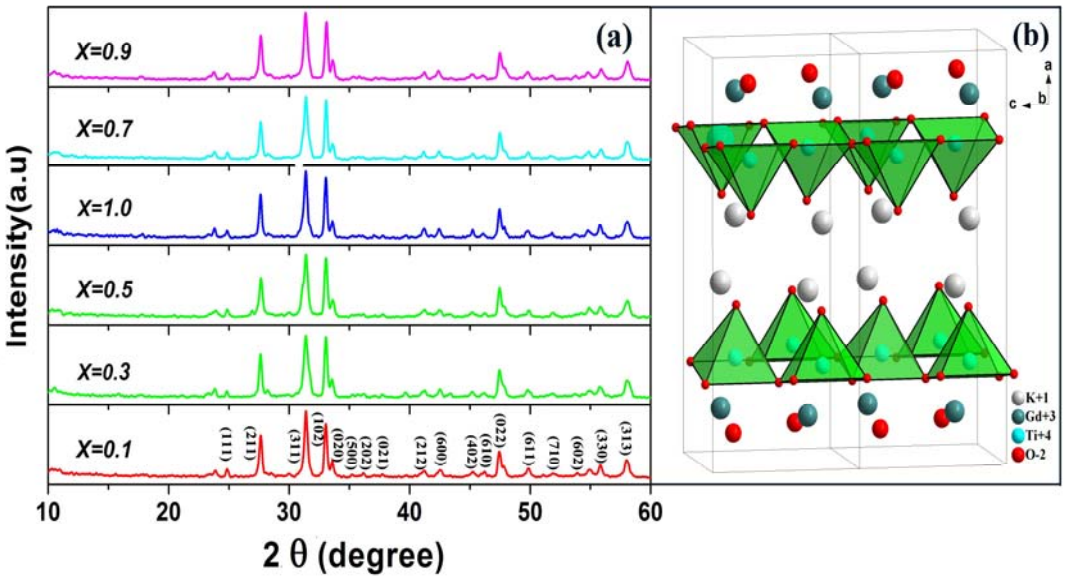

Fig.1 XRD patterns of samples $KGd_{1-x}Eu_xTiO_4$ with different Eu^{3+} concentrations (a) annealed at 800 ℃ for 3 h in air and the crystal structure of $KGdTiO_4$ (b).

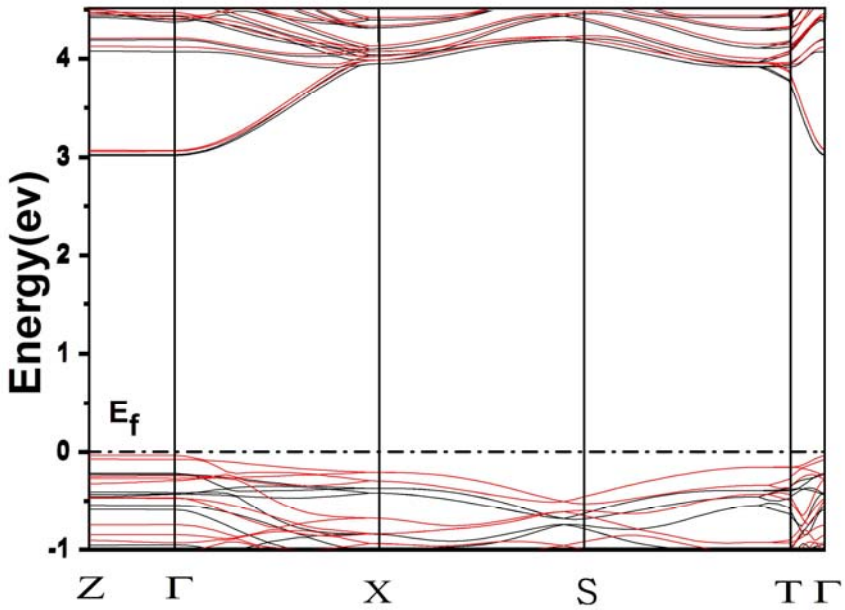

Fig.2 The calculated energy band structure of $KGdTiO_4$.

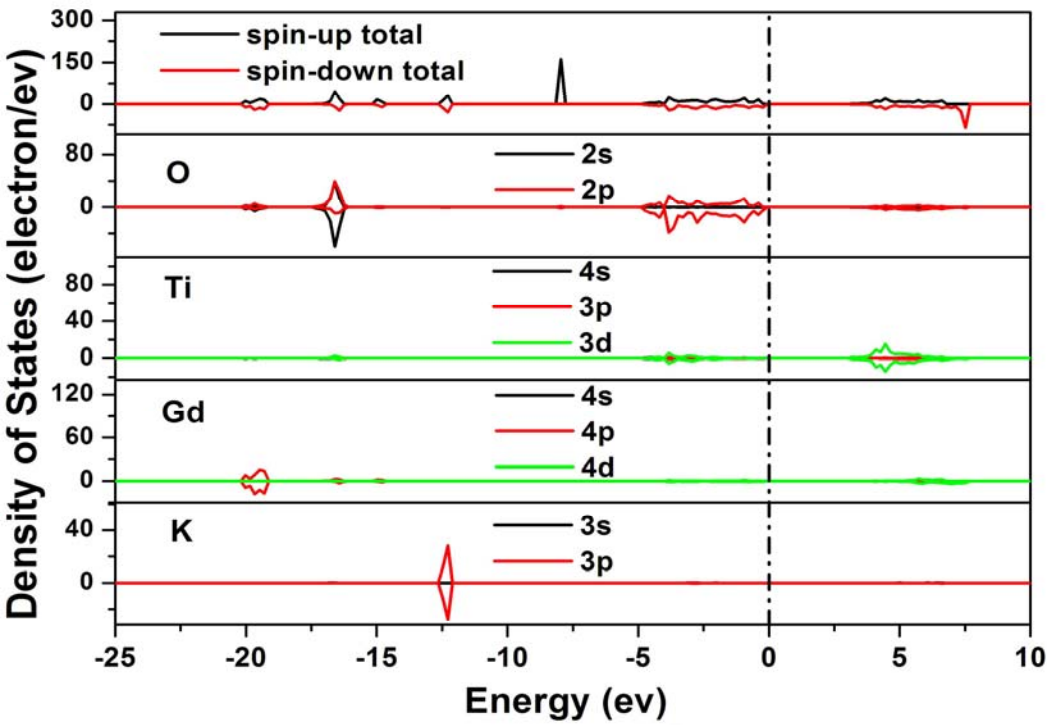

Fig.3 Density of states and partial DOS of $KGdTiO_4$ near the Fermi energy level (the Fermi energy is the zero of the energy scale).

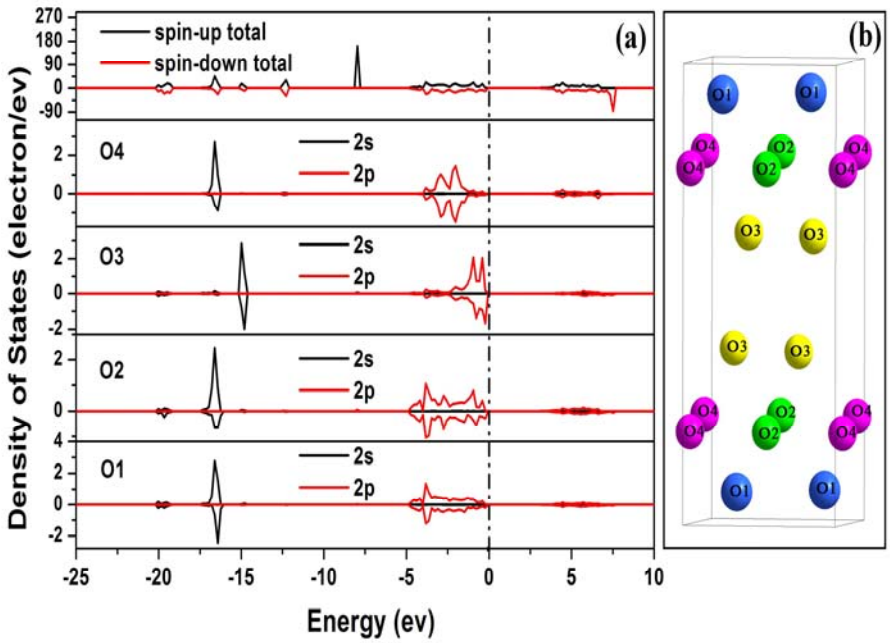

Fig.4 Density of states and O-DOS of $KGdTiO_4$ (a), the O-site of $KGdTiO_4$ in unit cell (b).

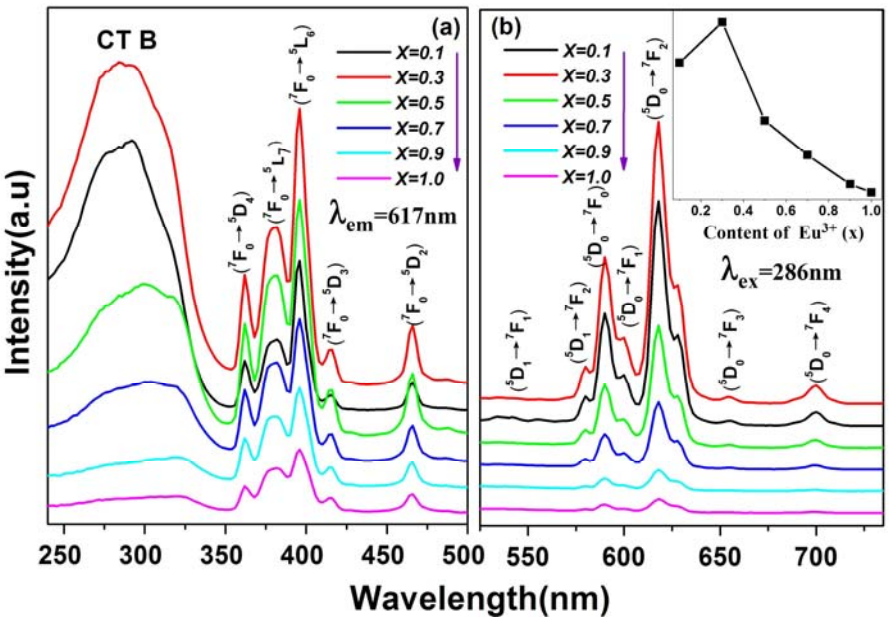

Fig.5 (a) PLE (λ_{em}= 617 nm) and (b) PL (λ_{ex}=286 nm) spectra of the phosphor $KGdTiO_4$:$x$$Eu^{3+}$ annealed at 800 ℃ for 3 h. Inset is the dependence of the PL intensities on the contents of Eu^{3+} (x).

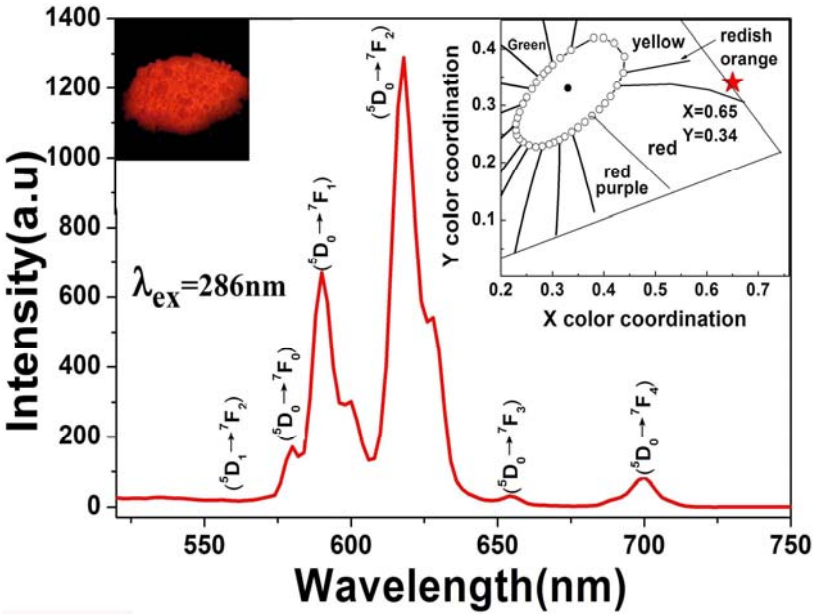

Fig.6 PL (λ_{ex}=287 nm) spectra of sample $KGd_{0.7}Eu_{0.3}TiO_4$ with its corresponding color coordinates (inset) luminescent photograph (left, *excited at 254 nm*).

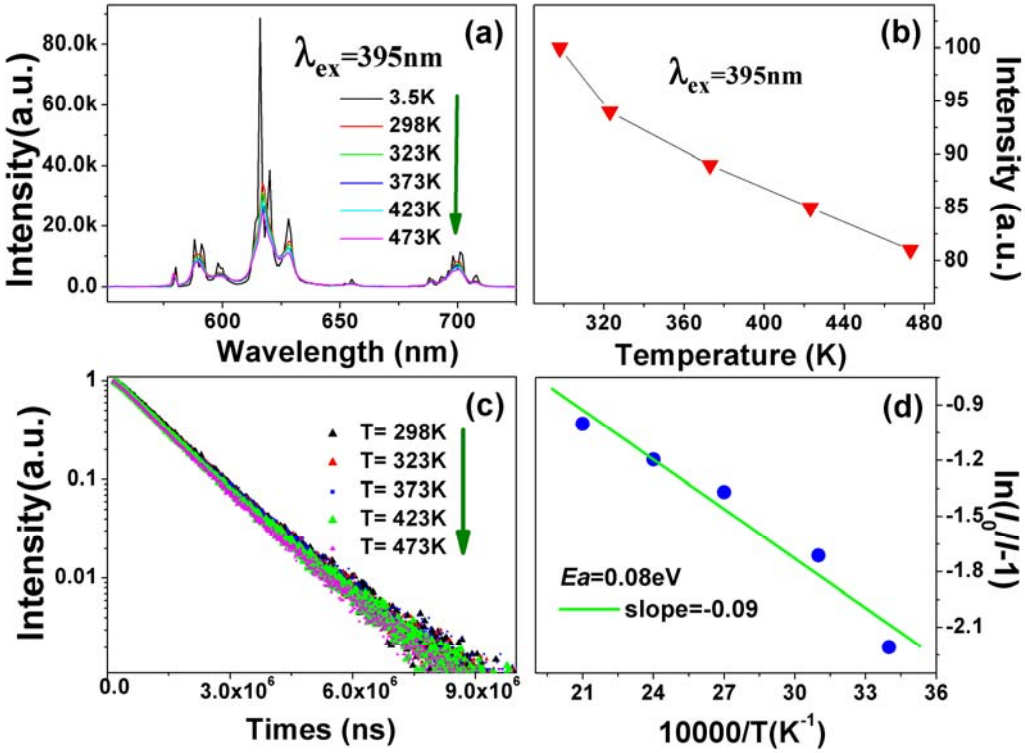

Fig.7 Temperature-dependent PL spectra of $KGd_{0.7}Eu_{0.3}TiO_4$ phosphors excited at 395nm (a). Normalized PL intensity of $KGd_{0.7}Eu_{0.3}TiO_4$ phosphors as a function of temperature (b). Decay curves of $KGd_{0.7}Eu_{0.3}TiO_4$ phosphors at different temperatures (c). Plot of $\ln[(I_0/I)-1]$ *vs*. 10000/T for phosphors $KGd_{0.7}Eu_{0.3}TiO_4$ (d).

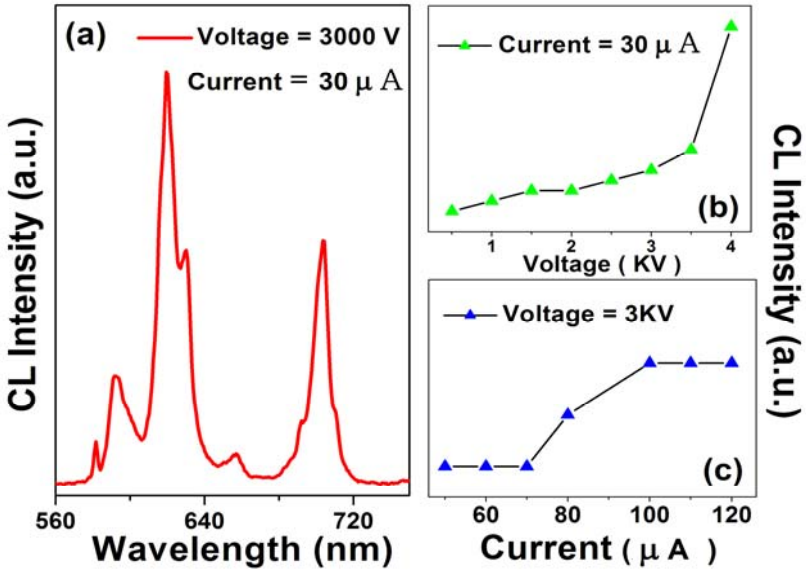

Fig.8 CL spectra of samples $KGd_{0.7}Eu_{0.3}TiO_4$ (a), the dependence of CL intensity on the accelerating voltage (b) and filament current (c).